Analytical Letters

ISSN: (Print) (Online) Journal homepage: www.tandfonline.com/journals/lanl20

Investigation of the Interaction of Monoamine Oxidase (MAO) Inhibitor Biscoumarins with Hemoglobin and Albumin Using Multi-Spectroscopic Techniques and Molecular Docking

Bengü Sema Mutafoğlu, Furkan Meletli & Özkan Danış

To cite this article: Bengü Sema Mutafoğlu, Furkan Meletli & Özkan Danış (21 Apr 2024): Investigation of the Interaction of Monoamine Oxidase (MAO) Inhibitor Biscoumarins with Hemoglobin and Albumin Using Multi-Spectroscopic Techniques and Molecular Docking, Analytical Letters, DOI: 10.1080/00032719.2024.2344071

To link to this article: https://doi.org/10.1080/00032719.2024.2344071

ANALYTICAL LETTERS
https://doi.org/10.1080/00032719.2024.2344071

Taylor & Francis
Taylor & Francis Group

BIOANALYTICAL

Investigation of the Interaction of Monoamine Oxidase (MAO) Inhibitor Biscoumarins with Hemoglobin and Albumin Using Multi-Spectroscopic Techniques and Molecular Docking*

Bengü Sema Mutafoğlu, Furkan Meletli, and Özkan Danış

Department of Chemistry, Faculty of Science, Marmara University, Istanbul, Türkiye

ABSTRACT

Coumarin and their derivatives, such as biscoumarins, which are found as active ingredients in a variety of drugs, possess a wide range of biological activities. In this paper, the inhibitory effects of biscoumarin derivatives B1 and B2 on monoamine oxidase (MAO) enzyme activity were studied. Their binding mechanism to bovine serum hemoglobin (BHb) and bovine serum albumin (BSA) was investigated using molecular docking and multi-spectroscopic methods such as absorption, fluorescence, and synchronized fluorescence spectroscopy. The fluorescence quenching processes were analyzed using the Stern-Volmer, Lineweaver-Burk, and Hill methods. In this regard, Stern-Volmer quenching constants (K_{sv}), Lineweaver-Burk constants (K_{LB}), and binding constants (K_a) were calculated at three temperatures (298, 310 and 322 K). The fluorescence studies showed that the binding of biscoumarins to BHb or BSA was a driven by static quenching. The K_a values of B2 to BHb and BSA (2179.11 and 18453.98 x 10^5 M^{-1}) was larger than B1 at corresponding temperature (62.75 and 599.90 x10^5 M^{-1} for BHb and BSA, respectively), which indicates that the affinity of B2 toward the proteins were higher than that of B1. Moreover, thermodynamic parameters explained that hydrogen bonds were the main binding force stabilizing the protein-ligand complexes. Additionally, molecular docking studies have revealed binding energies, ligand efficiency values, and interactions with amino acid residues of proteins. The results of these investigations may be helpful in analyzing drug-protein binding of biscoumarins for potential future applications.

ARTICLE HISTORY
Received 26 December 2023
Accepted 13 April 2024

KEYWORDS
Albumin; biscoumarin; hemoglobin; molecular docking; monoamine oxidase

Introduction

Compared to inorganic and/or synthetic molecules, natural products from herbal sources with high biocompatibility and low toxicity are important in the discovery of novel drug molecules (Osbourn and Lanzottia 2009). The laboratory derivatization of natural products can potentially enhance their pharmacological activities and contribute to the development of new therapeutic agents. Secondary metabolites of plants and their

CONTACT Furkan Meletli furkan.meletli@marmara.edu.tr Department of Chemistry, Faculty of Science, Marmara University, Istanbul, Türkiye.

*This study was presented at the 12th Aegean Analytical Chemistry Days at Yildiz Technical University, Istanbul, Türkiye, on October 19-22, 2023.

Supplemental data for this article can be accessed online at https://doi.org/10.1080/00032719.2024.2344071.

derivatives are important and rich sources for the discovery of new drug candidates (Li and Vederas 2009). In the last 30 years, half of new chemical formations are drugs derived from natural products, particularly secondary metabolites, which make up more than a quarter of the currently available drugs (Yeshi et al. 2022; Crane and Gademann 2016).

Coumarins are secondary plant metabolites, and they have been found to be present in natural structures such as fungi, bacteria and stems, fruits, and flowers of vascular plants (Lyndem et al. 2023). Coumarins are divided into four main classes: simple coumarins, furanocoumarins, pyranocoumarins, and coumarins with substitutions in the pyrone ring (Murray, Mendez, and Brown 1982). Biscoumarins, which belong to the latter class, are chemical structures formed as a result of the dimerization of 4-hydroxycoumarin through a bridge. Coumarins have been discovered to have various pharmacological properties such as anti-coagulant, anti-neurodegenerative, anti-bacterial, anti-oxidant, anti-diabetic, anti-depression and anti-cancer (Hudáčová́ et al. 2021). They carry out some of these pharmacological effects as enzyme inhibitors. Their inhibitory activities on enzymes such as glutathione-S-transferase, acetylcholinesterase, carbonic anhydrase, lipoxygenase, cyclooxygenase 2, alkaline phosphatase, monoamine oxidase, DNA polymerase β-lyase, α-glucosidase have been reported in the literature (Muratovıć́ et al. 2013; Orhan 2018). It is also known that biscoumarins have anticoagulant, antiviral, antiHIV, anti-pyretic, antimicrobial, anticancer, antithrombotic, antioxidant activities and possess inhibitory effects on K-562 proliferation, urease, and glucosidase enzymatic activity (Faisal et al. 2017).

Coumarin derivatives are important sources for the discovery of new, selective, and reversible monoamine oxidase (MAO) inhibitors. MAOs are flavoenzymes containing flavin-adenine-dinucleotide as a prosthetic group in the outer membrane of the mitochondria and catalyze the oxidation of neurotransmitters, which contain the amine functional group (Edmondson and Binda 2018; Ramsay and Albreht 2018). Depending on their substrate selectivity and inhibitor differences MAOs are classified into two isoenzymes, MAO-A and MAO-B. The substrates of MAO-A are serotonin and norepinephrine, while 2-phenylethylamine and dopamine are the substrates of MAO-B. Selective MAO-A inhibitors are used in the treatment of depression due to their suppressing action on the metabolism of serotonin and norepinephrine, while selective MAO-B inhibitors are used in Parkinson's (PD) and Alzheimer's (AD) diseases because they act by preventing the oxidation of dopamine in the central nervous system (Bekircan et al. 2022). Current treatment protocols for Parkinson's disease include the use of MAO inhibitors, such as selegiline, rasagiline, and safinamide (Tan, Jenner, and Chen 2022; Özdemir et al. 2021).

Many therapeutic drugs do not achieve the desired effectiveness due to limitations in stability, half-life, and solubility. It is recommended to use drug carrier systems to protect substances from degradation, ensure efficacy, and avoid immune system rejection (Özdemir and Özalp 1995). As drugs are absorbed into the body and transported to target tissues *via* blood, interaction with blood proteins such as hemoglobin and albumin is inevitable. Hemoglobin (Hb) has a critical role in the transport of oxygen and carbon dioxide throughout the body, as well as pH regulation, hydrogen peroxide dispersion and carrying electrons throughout the body (Quds et al. 2022; Gaurav et al. 2021).

Hb participates in transporting various exogenous and endogenous molecules, including drugs and natural products with biological activity (Shanmugaraj, Anandakumar, and Ilanchelian 2014; Peng et al. 2014; Basu and Suresh Kumar 2015). This interaction potentially causes conformational changes and altered function of hemoglobin. Hemoglobin is a tetrameric protein consisting of two α- (141 amino acid residues) and two β- (146 amino acid residues) polypeptide chains and four porphyrin rings (heme group) (Seal et al. 2018). Each α – β dimer contains 3 tryptophan (Trp) (α-14, β-15 and β-37) and 6 tyrosine (Tyr) amino acid residues that give Hb its intrinsic fluorescence (Ma et al. 2012). Serum albumin (SA), one of the most common proteins in the blood, has a primary function in the transport of endogenous and exogenous substances (fatty acids, drugs, metabolites, etc.), in addition to its different physiological functions such as adjusting osmotic pressure, determining blood pH, and reducing free radicals (Novo and Al-Soufi 2007; Farrugia 2010). SA is a globular single chain protein consisting of 582 amino acid residues and structurally three homologous domains as IB, IIA and IIIA (Mishra and Heath 2021). It has been shown that substances – especially drugs – are located mostly in subdomains IIA and IIIA of the primary binding sites of SA (Ghuman et al. 2005; Taheri et al. 2022). The intrinsic fluorescence emission of SA is caused by the presence of tyrosine (Tyr) and tryptophan (Trp) residues. While tyrosine residues are dispersed across the entire polypeptide chain, Trp213 and Trp134 are on the surface of subdomain IB and in the hydrophobic cavity of subdomain IIA, respectively (Hsieh et al. 2016).

Under normal conditions, a significant amount of hemoglobin is encapsulated within erythrocytes; on the other hand, a small fraction exists freely in plasma. However, in abnormal circumstances such as anemia, malaria, and thalassemia, the concentration of cell-free Hb in plasma rises. This cell-free Hb is particularly prone to interacting with various compounds in the blood plasma (Seal et al. 2017). Additionally, the abnormal accumulation of hemoglobin in neurons could potentially lead to the development of neurodegenerative disorders, such as PD and AD (Chowdhury et al. 2020). This accumulation may trigger oxidative stress and contribute to the degeneration of dopaminergic neurons, a characteristic of PD. The exact mechanisms underlying this association are still under investigation, but the presence of Hb within neurons suggests a potential role in the pathogenesis of PD (Freed and Chakrabarti 2016). Some diseases (such as liver and kidney illnesses) cause to reduce binding of drugs to SA due to changing of albumin concentrations and conformation (Yamasaki et al.2013). Understanding how a drug behaves in the body and its effects on disease conditions by determining its pharmacokinetic and pharmacological activity is crucial to providing effective treatment for patients. For these reasons, investigation of the binding properties of small molecules to optimal biomacromolecules is necessary, and it has an important field in biochemistry (Kaffash et al. 2024).

Previously, our group has reported the inhibitory effect of two novel biscoumarin derivatives on human glutathione S-transferase (Ozalp et al. 2023). In this study, inhibitory activity of biscoumarin derivatives on the monoamine oxidase enzyme was examined *in vitro*. Understanding the interaction between biscoumarin compounds and the carrier proteins albumin and hemoglobin is pivotal for comprehending their biophysical activity, as it has been established that they are pharmaceutically active

substances because of their ability to inhibit MAO and GST-transferase enzymes. In this context, the interaction mechanism of bovine serum albumin (BSA) and bovine hemoglobin (BHb) with biscoumarin derivatives were determined by multi-spectroscopic analysis and molecular docking, with a focus on binding constants, binding forces, binding sites, binding energies, and interaction type.

Experimental

Materials

Human MAO-A (*h*MAO-A), human MAO-B (*h*MAO-B), bovine hemoglobin (BHb), bovine serum albumin (BSA) and dimethyl sulfoxide (DMSO) were purchased from Sigma-Aldrich (St. Louis, MO, USA), and the Amplex Red MAO Assay Kit was purchased from Invitrogen (Waltham, MA, USA). All chemicals were of analytical grade. Ultrapure water was used in the preparation of all aqueous solutions. Synthesis route and spectral characterization of the biscoumarin derivatives were previously published (Ozalp et al. 2023). Absorbance and fluorescence spectrum of biscoumarins were given in Figures S1 and S2. BSA and BHb stock solutions were prepared in 20 mM phosphate buffer (pH 7.4). The stock solutions of biscoumarin derivatives were dissolved in DMSO.

Inhibition of in vitro hMAO-a and hMAO-B

Determination of the inhibitory activity of the biscoumarins on *h*MAO-A and *h*MAO-B isoenzymes was carried out using the Amplex Red Monoamine Oxidase Assay Kit by an *in vitro* continuous fluorometric method according to the manufacturer's instructions. The Amplex Red reagent (10-acetyl-3,7-dihydroxyphenoxazine) has great sensitivity and stability for H_2O_2, which is a product of p-tyramine, the common substrate for both MAO isoenzymes.

Biscoumarin derivatives were dissolved in DMSO to prepare a 10 mM stock solution, and their working concentrations were prepared from the stock. According to the Test Kit manual, 2 μL of inhibitor compounds dissolved in DMSO, 4.5 μL of *h*MAO-A or 4.5 μL of *h*MAO-B, and 93.5 μL 0.25 M pH 7.4 sodium phosphate buffer were added into the each well of the black flat-bottomed spectrofluorometric 96-well plates and incubated by stirring at 37 °C for 15 min in the dark fluorimeter chamber. After the incubation, 100 μL of substrate solution (200 μL 20 mM Amplex Red, 100 μL 200 U/ml horseradish peroxidase, 200 μL 100 mM p-tyramine in 9.5 mL 0.25 M pH 7.4 sodium phosphate buffer) was added, and the reaction was started. The progress of the enzymatic reaction was followed by taking measurements every 30 s for 15 min in a multi-measurement microplate fluorescence reader at 37 °C. Reactions carried out with *h*MAO-A and *h*MAO-B isoenzymes were allowed to run in parallel at the same time, and fluorescence intensities were determined subtracting the baseline fluorescence intensity from the observed fluorescence intensity at the end of 30 min. Assays were carried out the FLX800TM Fluorescence Reader (Bio-Tek Instruments., Winooski, VT, USA).

UV-Vis absorption spectroscopy

The absorption spectra of BHb and BSA in the absence and presence of biscoumarins were carried out in the range of 200–600 nm at 298 K. The concentration of BHb and BSA remained constant at 1.5×10^{-6} M against different concentrations of biscoumarins, which ranged from 5.00×10^{-6} to 50.00×10^{-6} M. The Thermo Scientific Helios Zeta Double Beam spectrophotometer (Thermo Fischer Waltham, MA, USA) was used to measure the absorption spectrum.

Fluorescence spectroscopy

Equipped with 1.0 cm quartz cells, the Varian Carry Eclips fluorescence spectrometer (Agilent, Santa Clara, CA, USA) was used for both fluorescence and synchronous fluorescence spectroscopy. The emission spectra were collected in the range of 290–600 nm with 280 nm excitation wavelength at three temperatures (298, 310 and 322 K) using 5.0 nm slit widths. The concentration of BHb and BSA remained constant and the same as in absorption studies against increasing concentrations of biscoumarins.

Synchronous fluorescence spectra were carried out through simultaneous scanning with a wavelength difference ($\triangle\lambda = \lambda_{em} - \lambda_{ex}$) of 15 nm ($\Delta$15) and 60 nm ($\Delta$60) to determine changes in the tyrosine and tryptophan microenvironments of BHb and BSA, respectively.

Fluorescence data was analyzed to determine changes in the hemoglobin and albumin structures and environments, along with quenching types, binding constants, and interaction details between the ligands and proteins. In the light of these information, the skeleton, secondary structure, and thermodynamic parameters such as enthalpy (ΔH^0), entropy (ΔS^0), and Gibbs free energy (ΔG^0) were defined.

Molecular docking

Molecular docking calculations were carried out using AutoDock 4.2 (The Scripps Research Institute Molecular Graphics Laboratory, La Jolla, CA, USA). The crystal structure of BHb and BSA was downloaded from the Protein Data Bank server (https://www.rcsb.org) PDB ID: 1G09 (resolution 2.04 Å) and PDB ID: 4F5S (resolution 2.47 Å), respectively (Zhang et al. 2012, Bawa et al. 2022). In the molecular docking studies, heteroatoms were deleted, polar hydrogen atoms were added, and the Kollman model was applied to the proteins (Seal et al. 2019). Molecular docking results were performed *via* the Lamarckian Genetic Algorithm (LGA).

Rotatable bonds were defined by determining the roots of the ligands with the help of AutoDock Tools (Morris et al. 2009). The Avogadro 1.2.0 (http://avogadro.cc/) was used in the preparation of ligands (Hanwell et al. 2012). The geometries obtained as a result of molecular docking were read in the appropriate file format in the Auto Dock4.2 software. During the docking process, grid was described as $70 \times 70 \times 70$ points with a grid spacing of as 0.375 Å and center of grid was defined with coordinates (x, y, and z) 1.07, 65.021, and 12.094 for BHb by using Autogrid4 (Lyndem et al. 2023).

The docking studies of BSA were carried out for each binding sites as IB (-4.795, 30.487, 101.007), IIA (10.906, 16.276, 119.720) and IIIA (19.857, 33.531, 97.915) and the

gridbox size was $60 \times 60 \times 60$ with same grid spacing. The molecular docking parameters were used as the program's default values: GA population size = 150, maximum number of energy evaluations = 2500000, GA crossover mode = two points, mutation, elision, and crossover 0.02, 1.0, and 0.8, respectively (Zhang et al. 2012). The lowest energy conformations of the compounds resulted from the docking were selected. Ligand interactions with proteins were examined and determined interaction types with amino acid residues using Discovery Studio 2021 Client (BIOVIA, 2021).

Results and discussion

MAO inhibition activities of biscoumarins

MAO inhibitory activity of the biscoumarin derivatives were determined from *in vitro* experiments. As noted in Table 1, biscoumarins showed MAO inhibitory activity at concentrations in the micromolar range. Although the only difference between the two biscoumarin derivatives is the hydroxyl (-OH) and acetoxy (-OAc) substituents on *p*- and *m*-positions at 3-aryl rings (Table 1), their activities were quite different. Hydroxy-substituted **B2** derivative exhibited relatively lower IC_{50} values than acetoxy-substituted **B1** for both *h*MAO-A and *h*MAO-B isozyme. Furthermore, while **B1** was selective to *h*MAO-B, **B2** was selective to *h*MAO-A. These shifts in the activity and selectivity of differently substituted biscoumarin derivatives were compatible with the data that we reported for the aryl coumarin derivatives in our previous publication (Yuce-Dursun et al. 2023). In that study, it was observed that -OH groups located at various positions on the coumarin core and 3-aryl ring increase the inhibitor activity and the selectivity for MAO-A. On the contrary, the acetoxy substitutions on the coumarin core and 3-aryl ring decrease the activity and shift the selectivity toward MAO-B. These results were attributed to the presence of the -OH group as a hydrogen bond donor.

Table 1. Structures, IC_{50} values and selectivity index (SI) of the biscoumarin derivatives for MAO-A and MAO-B.

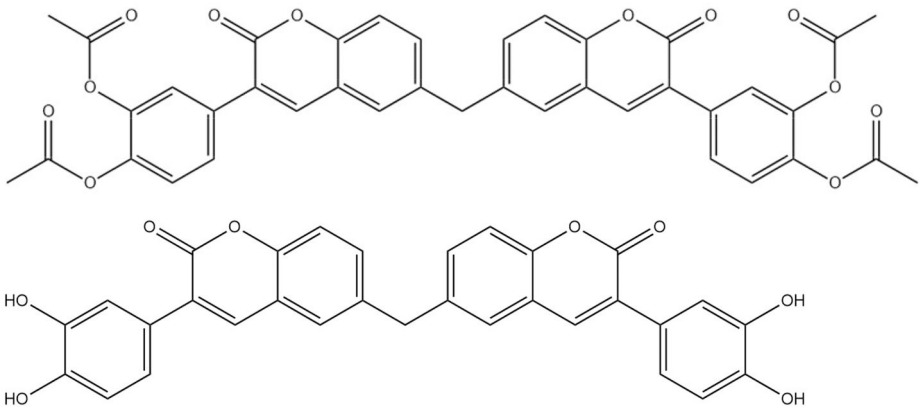

Compound	MAO-A (IC_{50} μM)	MAO-B (IC_{50} μM)	*SI (A/B)
B1	24.22 ± 0.309	18.63 ± 0.211	1.30
B2	1.82 ± 0.056	3.75 ± 0.171	0.49

*Each IC_{50} value given as the mean ± S.D. of three replicate experiments.

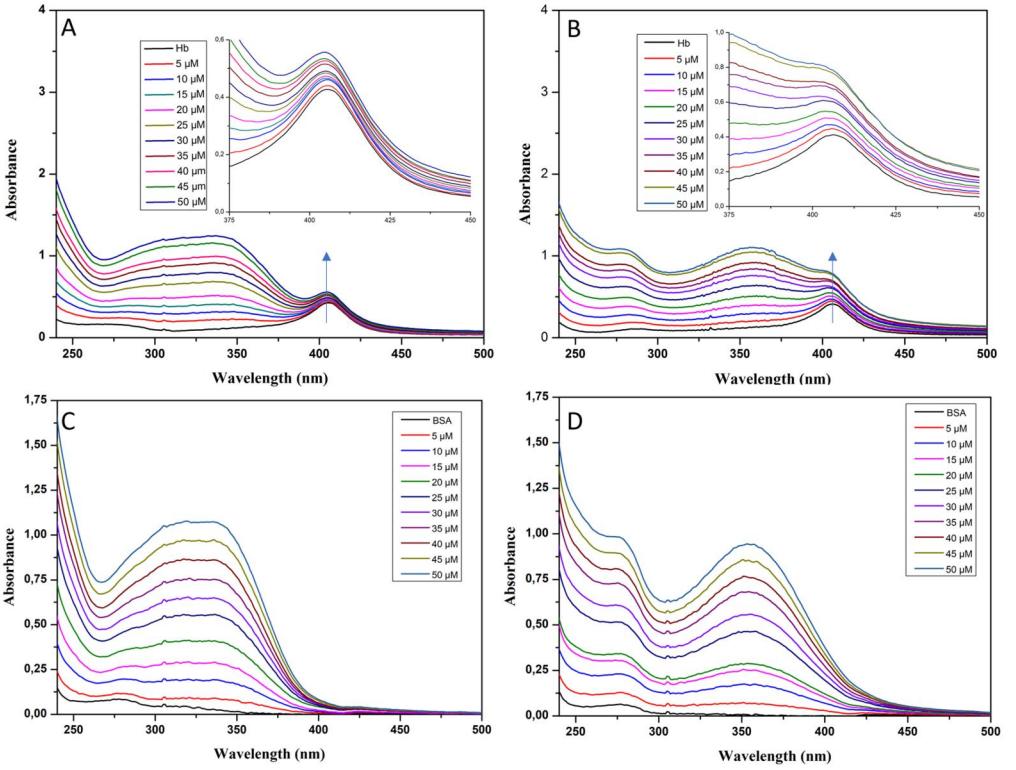

Figure 1. Absorption spectra of (a) BHb-B1; (b) BHb-B2; (c) BSA-B1; and (D) BSA-B2 complexes. Conditions: BHb and BSA 1.5 μM, B1 and B2 concentrations 5–50 μM, at $T = 298$ K, pH 7.4.

UV–vis spectra of the biscoumarins with BHb and BSA

UV–Vis absorption measurement is a very simple and effective method to explore structural changes of protein and the protein-ligand complex. Figure 1 shows the absorption spectra of BHb and BSA with the increased concentrations of biscoumarin derivatives. While Hb demonstrates two characteristic peaks at 280 and 405 nm, representing the absorption peaks of aromatic amino acid residues (phenylalanine, tyrosine, and tryptophan) and the porphyrin ring (Yang et al. 2012), BSA has only one distinctive peak at 280 nm which was mainly caused both by the pi-pi* transitions of aromatic amino acid residues (Bawa et al. 2022).

The absorption spectra of BHb and BSA at 280 nm increased with the addition of increasing concentrations of **B1** and **B2** (**BHb-B1/B2** and **BSA-B1/B2**) (Figure 2). This result indicated that biochemical interactions occurred between biscoumarin derivatives and aromatic residues of BHb and BSA. These interactions are probably the outcome of the BHb's and BSA's changing skeleton as well as the exposure of aromatic amino acid residues in the internal hydrophobic area (Wang et al. 2010; Tunç, Duman, and Bozoğlan 2013). Eventually, the increases in the absorption peaks attributed to the interaction of BHb and BSA with **B1** and **B2** as an effect of ground state complex formation (Yu, Cai, et al. 2022).

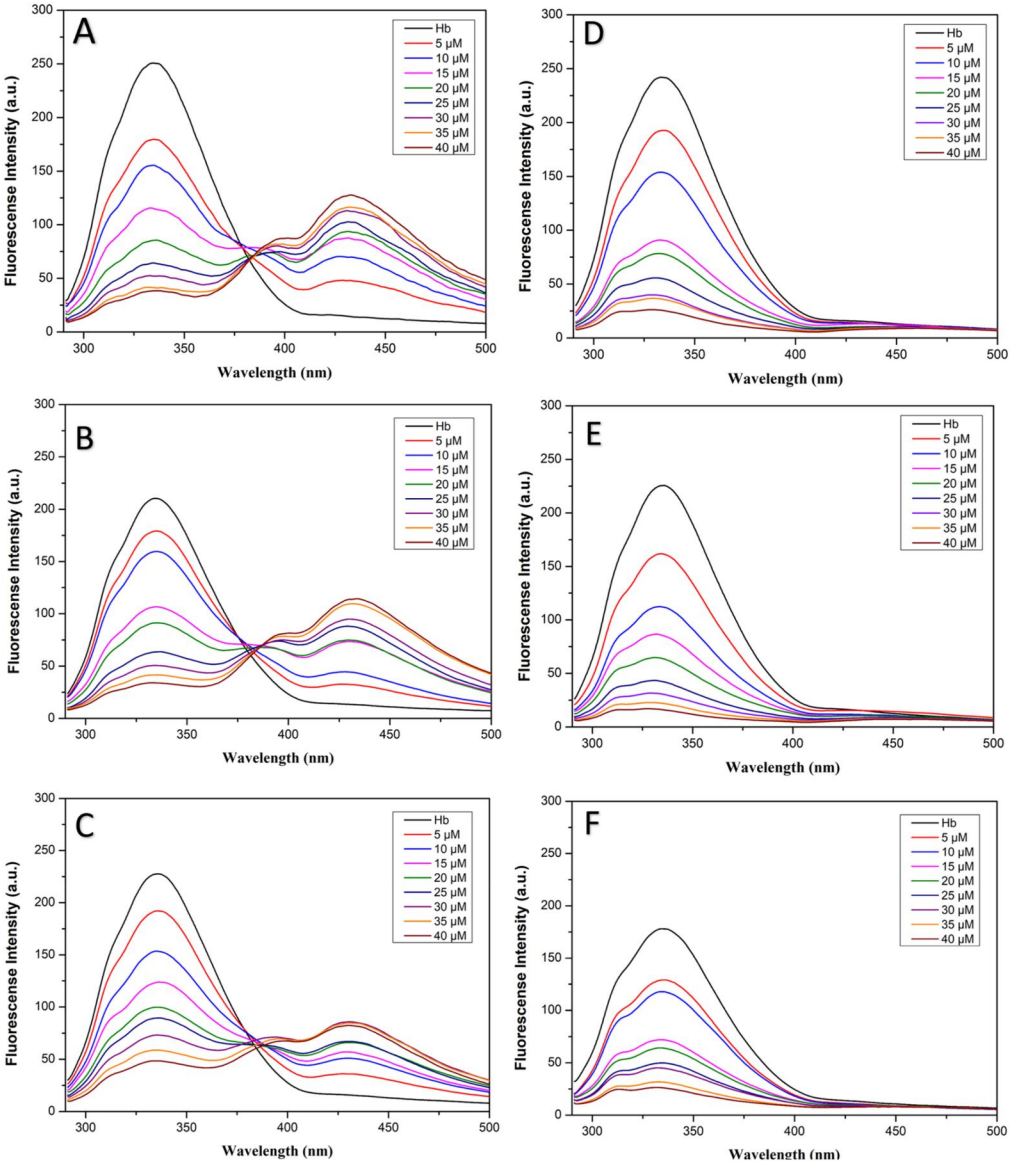

Figure 2. Fluorescence spectra of BHb (1.5 μM) with various concentrations of B1 and B2. (a) BHb-B1 at 298, (b) BHb-B1 at 310, (c) BHb-B1 at 322 K, and (d) BHb-B2 at 298, (e) BHb-B2 at 310, and (f) BHb-B2 at 322 K.

The characteristic peak of the heme Soret band of BHb at 405 nm are shown in Figure 1a,b. The Soret band appears due to the pi-pi* electron transition in the heme group embedded in hydrophobic pockets formed by non-polar amino acids Val, Leu, Phe, Trp, etc. (Kaur et al. 2023). We have suggested that the increasing of absorbance intensity was observed because of the release of the heme group from the hydrophobic cavity of BHb. **BHb-B1** and **BHb-B2** (**BHb-B1/B2**) formation may be in the native heme orientation, inducing the spread of peptide chains in BHb and integrating them into hydrophobic

pockets (Zolghadri et al. 2010). Compound **B2** caused a greater increase in the Soret peak of BHb compared to **B1**. Therefore, we indicated that result of difference interaction of the compounds with amino acid residues such as Val causes further conformational changes in the hydrophobic pocket where the heme group is embedded. Moreover, we proposed that both compounds do not directly target or attack the heme molecule based upon the absence of notable change in the Soret peak (Yang et al. 2012).

Fluorescence spectroscopy

The presence of tryptophan, tyrosine and phenylalanine within the protein's structure leads to the generation of intrinsic fluorescence. The tryptophan residues contribute significantly to the observed fluorescence of hemoglobin and albumin. The primary source of hemoglobin's fluorescence is identified as the β-Trp37 residue located at the $\alpha_1\beta_2$ interface rather than the surface-located α–Trp14 and β–Trp15 residues (Bhuiya, Chowdhury, and Das 2019). Conversely, the intrinsic fluorescence of albumin is caused by the presence of two major tryptophan residues, Trp213 and Trp134, which are located in separate binding pockets (Topală et al. 2014).

Free hemoglobin and albumin exhibit a characteristic emission maximum in the 335 nm and 340 nm region upon excitation at 280 nm (Chowdhury et al. 2020; Yu, Cai, et al. 2022). The emission of hemoglobin and albumin complexed with the increasing concentration of ligands decreases compared to free proteins. Decreasing of the emission intensity of hemoglobin and albumin shows that the ligands bind in the region close to Trp residues, especially the $\alpha 1\beta 2$ interface of BHb (the central cavity of Hb including β-Trp37 residue), and subdomain IB or IIA of BSA (Lyndem et al. 2023; Hsieh et al. 2016). The conformational changes observed in BHb and BSA upon ligand binding are highly sensitive to microenvironmental changes of Trp residues and alter the intrinsic fluorescence of the protein. Studying the emission spectra and alterations in the fluorophores of them enables a grasp of the protein's dynamics and secondary structure.

The fluorescence spectra of BHb and BSA with the increasing concentrations biscoumarins **B1** and **B2** at different temperatures are shown in Figures 2 and 3, respectively. The fluorescence intensities of the BHb at 335 nm and BSA at 339 nm were quenched gradually in the presence of increasing concentrations of the biscoumarins at 298, 310 and 322 K. The interaction of biscoumarins with BHb and BSA quenched their intrinsic fluorescence. The quenching was evidence that a biochemical interaction between both compounds and the Trp residues of the BHb and BSA occurred, and it caused conformational modifications to protein structure.

Moreover, isosbestic points were observed in Figures 2a,b and 3a,b, indicating the equilibrium of **B1** with BHb and BSA and the complex formations in a 1:1 ratio (Chatterjee and Kumar 2016). In addition to that, complex formation occurred in a reversible manner, as can be understood from isosbestic points (Taheri et al. 2022). While no significant shift in the BHb's fluorescence spectrum was observed for both compounds, a slight blue shift was seen in the fluorescence spectra of BSA with **B1** and **B2**. These results show that, with the binding of ligands, tryptophan regions of BSA became more hydrophobic as a consequence of the changing polarity of the microenvironment. Synchronized fluorescence studies were performed to better understand microenvironmental changes in BHb.

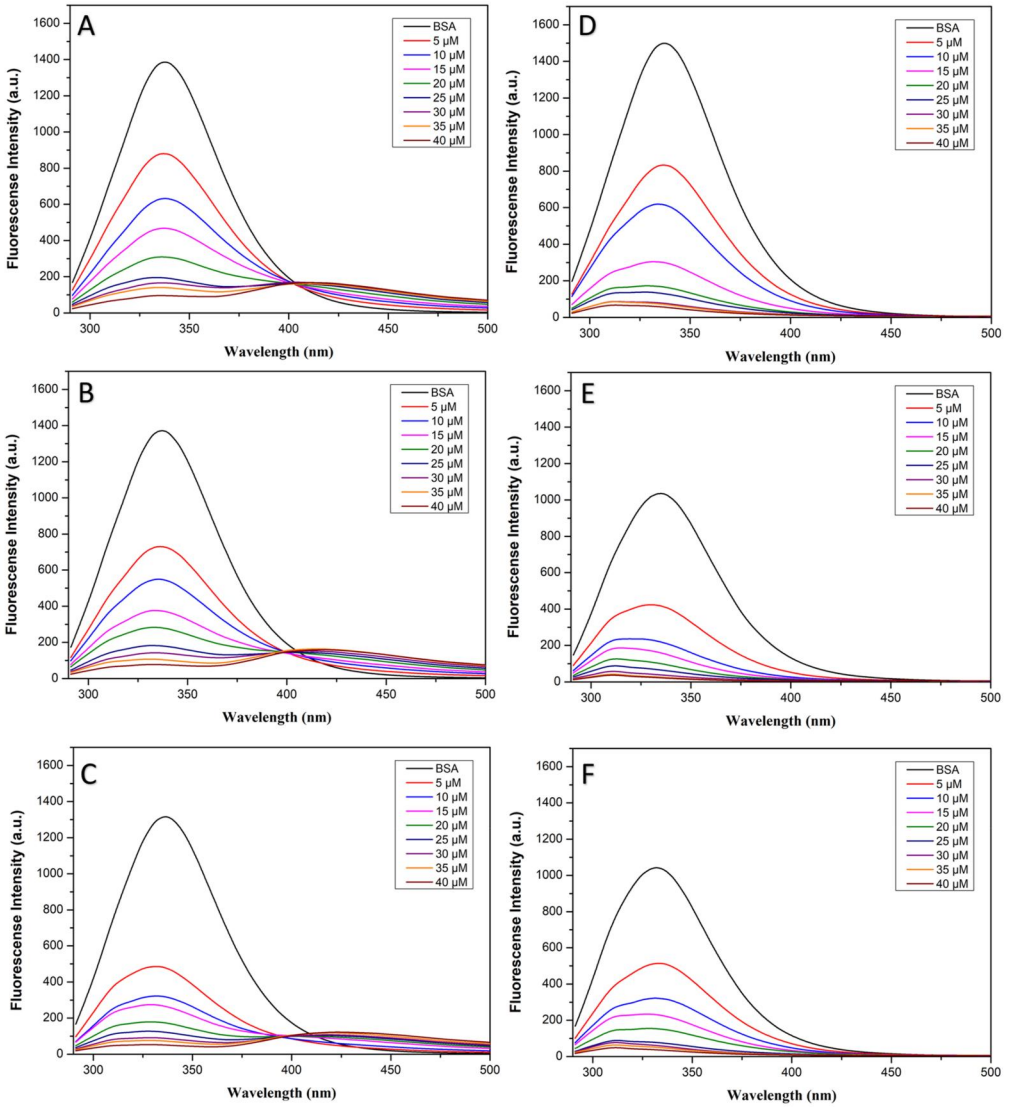

Figure 3. Fluorescence spectra of BSA (1.5 μM) with various concentrations of B1 and B2. (a) BSA-B1 at 298, (b) BSA-B1 at 310, (c) BSA-B1 at 322 K, and (d) BSA-B2 at 298, (e) BSA-B2 at 310, and (f) BSA-B2 at 322 K.

Synchronous fluorescence

Synchronized fluorescence spectra shows the conformational changes in the microenvironments of aromatic amino acid residues of proteins that occur with ligand binding. Δ15 nm difference between the excitation and emission wavelengths indicates the focus on the protein's tyrosine region, while Δ60 nm difference points to the protein's tryptophan region (Quds et al. 2022). The synchronized fluorescence spectroscopy was recorded by progressively increasing the concentrations of **B1** and **B2** while maintaining a constant BHb and BSA concentration in Figures 4 and 5.

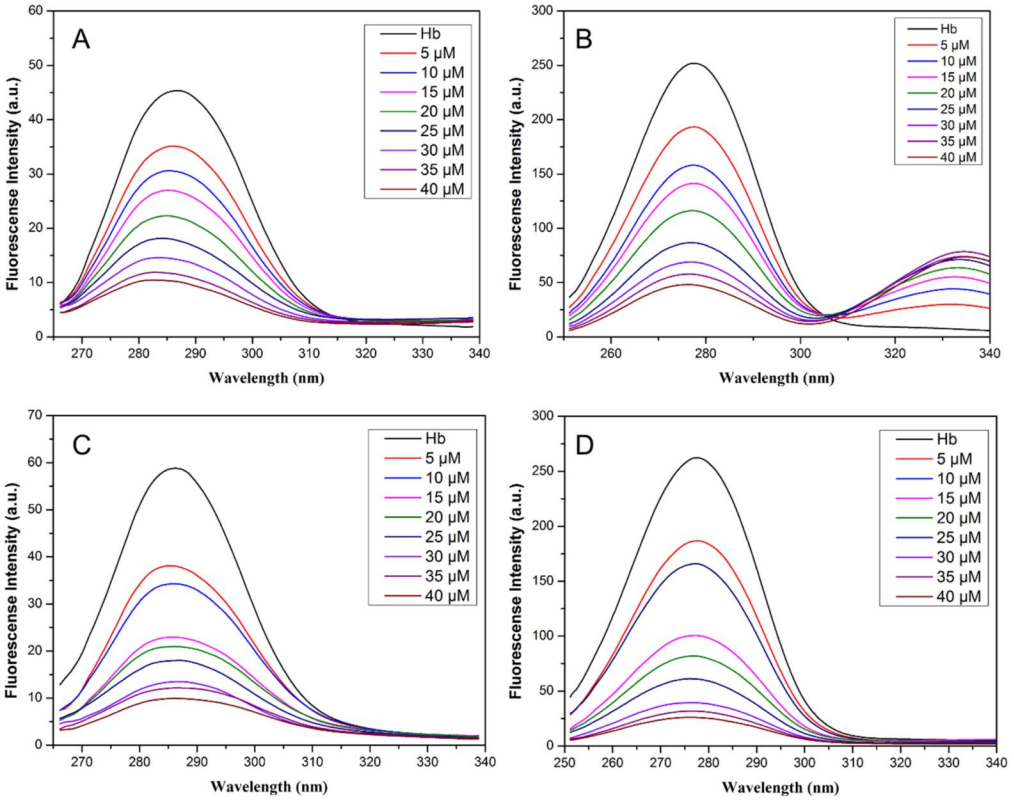

Figure 4. Synchronous fluorescence spectra of (a) BHb-B1, △15 nm; (b) BHb-B1, △60 nm; (c) BHb-B2, △15 nm; and (d) BHb-B2, △60 nm complexes. Conditions: Hb 1.5 μM and B1-B2 concentrations 5–40 μM at 298 K and pH 7.4.

The fluorescence spectra of **BHb-B1** and **BHb-B2** were similar and there was a decrease in the fluorescence intensities with the addition of separate **B1** and **B2**. There was no significant change of shift in the △60 nm spectrum with the addition of ligands, but there was a slight blue shift in the Δ15 nm spectrum of the **B1** compound. We suggest that the tyrosine sites in BHb were more accessible for **B1,** and that interactions with these sites were more likely. The blue shift in the spectrum showed that the polarity in the microenvironment of the tyrosine region decreased. When the synchronized fluorescence spectra of **BSA-B1** and **BSA-B2** were examined, the decreasing trend of the fluorescence intensities of BSA with the addition of compounds for both spectra were seen. A greater decline occurred in the △60 nm spectrum of the tryptophan regions of BSA for both compounds. Similar to the hemoglobin studies, a blue shift was observed at the Δ15 and Δ60 nm spectra for **BSA-B1**, whereas no change was observed in the spectra of compound **B2**. This shift seen for compound **B1** was evidence of a change in the microenvironment of the tyrosine and tryptophan amino acid residues.

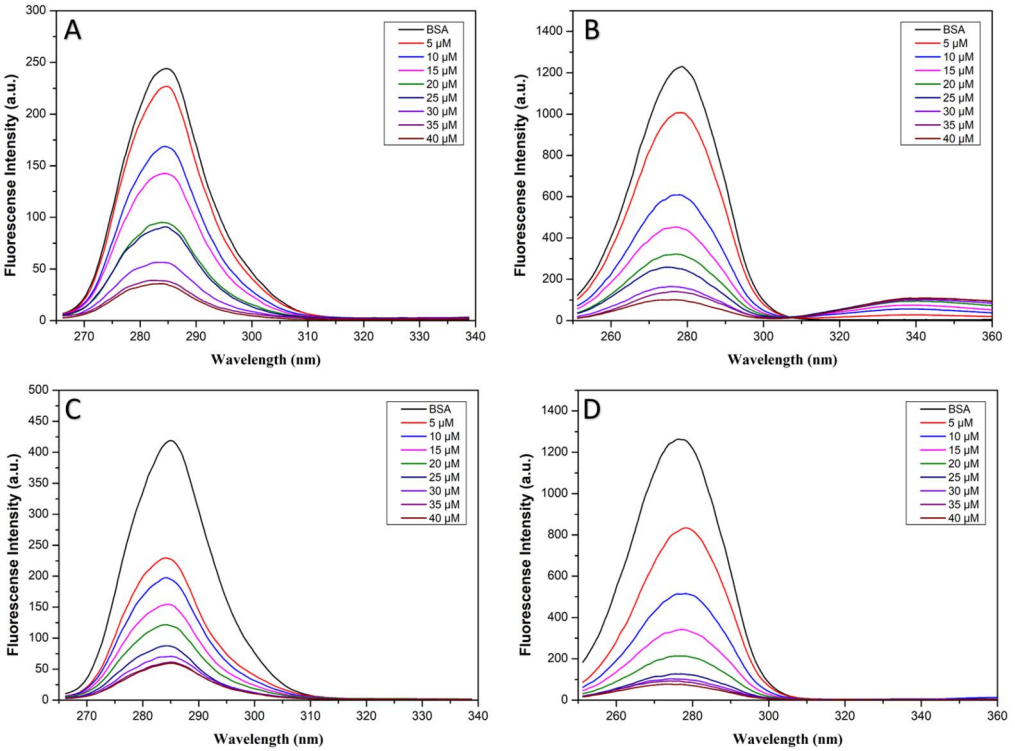

Figure 5. Synchronous fluorescence spectra of (a) BSA-B1, △15 nm; (b) BSA-B1, △60 nm; (c) BSA-B2, △15 nm; and (d) BSA-B2, △60 nm complexes. Conditions: Hb 1.5 μM and B1-B2 concentrations 5–40 μM at 298 K and pH 7.4.

Quenching mechanism of BHb and BSA by biscoumarins

Fluorescence quenching has been widely studied to obtain information about biochemical systems. Quenching can occur with various reasons, such as excited-state reactions, molecular rearrangements, energy transfer, ground-state complex formation, and collisional quenching (Lyndem et al. 2023). There are three forms of fluorescence quenching mechanisms: dynamic (collisional), static (ground-state complex formation), and mixed (both static and dynamic). For either static or dynamic quenching requires contact between the fluorophore and quencher (Lavanya et al. 2023).

Fluorescence quenching data were analyzed by the Stern-Volmer equation to determine the separately quenching parameters of BHb and BSA with **B1** and **B2**:

$$F_0/F = 1 + k_q\tau_0[Q] = 1 + K_{sv}[Q] \quad (1)$$

where F_0 and F are the fluorescence intensity of BHb with and without the quencher, respectively; k_q is the bimolecular quenching constant; τ_0 is the lifetime of the biomolecule (10^{-8} s), K_{sv} is the Stern–Volmer quenching constant, and [Q] is the concentration of quencher (Seal et al. 2019).

Quenching mechanism can be determined according to the K_{sv} values of the protein with quencher. When the K_{sv} value increases with temperature, the quenching type is determined as dynamic, while in static quenching, the K_{sv} value remain constant or

decrease with increasing temperature. The rationale here lies in the principle that elevated temperatures prompt swifter diffusion, consequently leading to a heightened occurrence of collisional quenching, where molecular collisions impact the fluorescence process (Lakowicz 2006).

Figure S3 shows the Stern-Volmer plots for **BHb-B1/B2** and **BSA-B1/B2** interactions, respectively. The plots displayed an upward curvature, concave toward the y-axis. The values of the binding parameters K_{sv}, k_q and R were determined by calculating the slope of the linear curve at 298, 310 and 322 K were listed in Table 2.

Based on the K_{sv} values of **BHb-B1/B2**, static quenching was indicated by the curves of 298–322 K. On the other hand, the curves of 298–310 K imply that the quenching type was dynamic. These findings corroborated one another as the curve is nonlinear. Therefore, we propose that a mixed quenching mechanism formation occurs for the **BHb-B1** and **B2** complexes. The K_{sv} values of **BSA-B1** increased consistently with temperature, suggesting dynamic quenching. Similar to BHb studies, the **BSA-B2** complex constants, when analyzed through the relationships 298–310 K and 298–322 K, demonstrated dynamic quenching. However, the 310–322 K relationship may alternatively be due to static quenching. Consequently, we assert that the quenching of BSA with **B1** and **B2** involved a mixed quenching mechanism.

In addition, the absorption spectra of BHb and BSA with **B1** and **B2** provide information about quenching type. Because dynamic quenching exclusively takes place within the excited states of the fluorophore, it does not impact the absorption spectrum of the fluorophore (Lavanya et al. 2023). This suggests that quenching is not only from dynamic collision but also by the formation of a ground state complex (Wang et al. 2010).

The fluorescence quenching data were analyzed according to the Lineweaver Burk equation, which is commonly reported to describe quenching mechanisms (Ali et al. 2022):

$$(F_0 - F)^{-1} = {F_0}^{-1} + {K_{LB}}^{-1}{F_0}^{-1}[Q]^{-1} \quad (2)$$

where K_{LB} is the effective quenching constant in the ground state.

The plot of $1/(F_0 - F)$ vs. $1/[Q]$ was applied to **BSA-B1/B2** and **BHb-B1/B2** complexes as shown in Figure S2. The binding constants (K_{LB}) of **B1** and **B2** at 298, 310 and 322 K are in Table 2. The observation of improved linearity in the comparison

Table 2. Parameters computed from both Stern-Volmer and Lineweaver-Burk relationships for BHb and BSA with B1/B2 complexes at different temperatures.

Compound	T (K)	K_{sv} x 10^5 (M^{-1})	k_q x 10^{13} (M^{-1} s^{-1})	R^2	K_{LB} x 10^4 (M^{-1})	R^2
BHb-B1	298	1.09	1.09	0.9705	4.30	0.9932
	310	1.37	1.37	0.97521	7.10	0.9557
	322	0.77	0.77	0.9835	1.40	0.9924
BHb-B2	298	1.69	1.69	0.9585	2.10	0.9868
	310	2.37	2.37	0.9240	5.10	0.9969
	322	1.22	1.22	0.9737	5.92	0.9151
BSA-B1	298	2.61	2.61	0.9544	8.48	0.9965
	310	3.26	3.26	0.9449	14.68	0.9793
	322	4.93	4.93	0.9539	2.80	0.9671
BSA-B2	298	5.39	5.39	0.9533	11.24	0.9721
	310	9.36	9.36	0.9125	24.99	0.9966
	322	5.70	5.70	0.9389	1.80	0.9971

between Stern Volmer curves proposed that the quenching mechanisms of both ligands are static (Alanazi and Abdelhameed 2016). All of these investigations have shown that additional data are required in order to identify the predominant type of quenching.

The bimolecular quenching constant (k_q) is another parameter to estimate the quenching mechanism. The k_q values were calculated for **BHb-B1/B2** and **BSA-B1/B2** complexes as 10^{13} $M^{-1}s^{-1}$ using the equation "$K_{sv} = k_q\tau_0$". Since the k_q values at 298, 310 and 322 K were higher than the maximum scatter collision quenching constant of various quenchers (2×10^{10} $L{\cdot}M^{-1}$ s^{-1}) in an aqueous medium, this indicated that probable quenching mechanism of BHb with biscoumarins occur as static quenching. Based on these k_q values, Lineweaver Burk curves and UV plots of biscoumarin, we determined that the result of predominant quenching type was static for all protein-ligand complexes (Ali et al. 2022).

Binding constants and number of binding sites

The double logarithmic Eq. (3) was utilized to compute the binding constants (K_a) and number of binding sites (n) of the biscoumarins with BHb and BSA in order to assess the efficiency of their interactions and quenching (Yang et al. 2012).

$$\log\left[(F_0 - F)/F\right] = \log\ K_a + n\log[Q] \tag{3}$$

The values of K_a and n for the interaction between BHb/BSA and biscoumarins were calculated from a plot of log[(F_0-F)/F] versus log[Q] as shown in Figure S3. The summary of the results is provided in Table 3. These results show that within the studied temperature range, the value n of the **BHb-B1** and **BSA-B1** complex were close to 1, indicating that **B1** has a single high affinity binding site for BHb and BSA. The isosbestic points observed in the fluorescence spectrum were explained by this investigation. However, the n values of the **BHb-B2** and **BSA-B2** complexes were close to 2, indicating that proteins may have two affinity binding sites for **B2.** The n values of **B1** and **B2** decreased with temperature due to a reduction in the stability of the protein-ligand complexes.

In the literature, n is also known as the Hill coefficient (n_H). The Hill coefficient is used to explain cooperativity in biochemistry. If the n_H value is greater than 1, it indicates positive cooperation between the protein and the ligand. On the contrary, the

Table 3. Binding constants (K_a) and number of binding sites (n) for BHb and BSA with B1/B2 complexes at different temperatures.

Compounds	Temperature (K)	K_a x 10^5 (M^{-1})	n	R^2
BHb-B1	298	62.75	1.40	0.9686
	310	75.27	1.39	0.9564
	322	55.94	1.41	0.9949
BHb-B2	298	2179.11	1,69	0.9855
	310	1784.88	1.65	0.9716
	322	39.26	1.34	0.9492
BSA-B1	298	599.90	1.53	0.9756
	310	290.33	1.44	0.9585
	322	72.52	1.27	0.9433
BSA-B2	298	18453.98	1.79	0.9713
	310	10678.25	1.69	0.9629
	322	4978.06	1.66	0.9645

opposite case shows negative cooperation (Liu et al. 2012). For both biscoumarins, *n* values greater than 1 obtained indicate that the interactions have positive cooperativity.

K_a values of **B1** and **B2** were calculated to be approximately 10^5, indicating strong binding between the biscoumarins and BHb and BSA. Thus, we predict that biscoumarins are able to demonstrate *in vivo* binding to both BHb and BSA (Abdollahpour et al. 2016). As the temperature increases, K_a values decrease (except **BHb-B1** at 310 K), suggesting that the stability of complexes decreases with the temperature. This phenomenon confirmed that the quenching mechanisms of BHb and BSA by the biscoumarins are static quenching (Buddanavar and Nandibewoor 2017).

Furthermore, when the K_a constants were compared, the K_a value of compound **B2** was much higher than compound **B1,** showing that it bonded to the proteins with high affinity. Moreover, both biscoumarins bonded to albumin with higher binding constants instead of hemoglobin. Since the acceptable constants of drug-protein complexes *in vivo* are in the range of 10^4 and 10^6 M^{-1}, these proteins are more appropriate to use as a **B1** carrier, especially hemoglobin, which would be a better transporter (Anjomshoa et al. 2015).

Thermodynamic parameters and the nature of binding forces

Molecular interactions involved in the binding of biomolecules with small molecules include hydrogen bonding, electrostatic, van der Waals interactions, and hydrophobic forces. Molecular interaction between the biscoumarins and BHb can be predicted based on magnitudes of the thermodynamic parameters, such as free energy changes (ΔG^0), enthalpy changes (ΔH^0), and entropy changes (ΔS^0). Thermodynamic parameters were calculated using the following equations to determine the interaction forces in the complexes (Liu et al. 2018).

$$\Delta G^0 = -RT\ \ln\ K \tag{4}$$

$$\Delta G^0 = \Delta H^0 - T\Delta S^0 \tag{5}$$

$$\ln(K_2/K_{1)} = (1/T_1 - 1/T_2)x\left(\Delta H^0/R\right) \tag{6}$$

where R is the gas constant.

The interaction forces between protein and ligands are electrostatic interactions if the values of ΔH^0 and ΔS^0 are negative and positive, respectively (Dohare et al. 2020). In another case, hydrogen bonding and van der Waals forces predominate in complexes if both ΔH^0 and ΔS^0 are negative (Alanazi and Abdelhameed 2016). The presence of hydrogen bonds between the ligands and proteins may contribute to the negative ΔH value of the system (Lehrer 1971). Furthermore, a positive value of ΔS^0 serves as evidence that increased randomness with binding results from hydrophobic interactions (Shahabadi et al. 2011).

The thermodynamic parameters for the binding interaction of biscoumarins with BHb and BSA are shown in Table 4. The negative values of ΔG^0 indicate that the interaction of biscoumarins with BHb and BSA was spontaneous. The **BSA-B2** complex, characterized by the smallest ΔG^0 value, exhibited greater stability compared to all complexes. Since all ΔH^0 values were negative, the binding processes were exothermic and driven by hydrogen bonds for all protein-ligand complexes. The positive and negative

Table 4. Thermodynamic parameters of BHb and BSA with B1/B2 complexes at three temperatures.

Compound	T (K)	ΔH^0 (kj mol^{-1})	ΔS^0 (j mol^{-1} K^{-1})	ΔG^0 (kj mol^{-1})
	298	−3.822	117.305	−38.779
BHb-B1	310	–	–	−40.186
	322	–	–	−41.594
	298	−519,336	−1592.824	−44.674
BHb-B2	310	–	–	−35.117
	322	–	–	−25.560
	298	−69.913	−84.718	−44.667
BSA-B1	310	–	–	−43.651
	322	–	–	−42.634
BSA-B2	298	−43.439	−31.973	−52.967
	310	–	–	−53.351
	322	–	–	−53.735

differences in ΔS^0 explain whether the other important dominant forces in binding were van der Waals or hydrophobic interactions. Accordingly, the binding of **BHb-B1** and **BSA-B2** complexes were in the direction of entropy and driven by hydrophobic interactions, while for **BHb-B2** and **BSA-B1**, the reactions were enthalpy-driven and dominated by van der Waals interactions.

Molecular docking

Molecular docking was used to simulate the interactions and binding modes of BHb and BSA with the biscoumarins. The simulated result of 10 conformations with different binding energies and ligand efficiency values were determined for each compound. By selecting the lowest energy conformations of the compounds, their interactions with amino acid residues of hemoglobin and albumin were examined, and the types of these interactions are provided in Figures 6 and 7. The docking studies of BHb show that the biscoumarin structures formed hydrogen bonds and non-covalent interactions with amino acid residues in the α_1 (A), β_1 (C), and β_2 (D) chains of hemoglobin. Both compounds were determined to localize in the central hydrophobic cavity of the BHb, and most of the amino acids residues that interact with the biscoumarins were the same, which include, α_1-Lys99, α_1-Lys127, β_1-Ala123, β_2-Pro36, α_1-Arg141, and β_2-Trp37. The interaction type of the β_2-Trp37 residue is pi-pi T-shaped, which occurs between the benzene rings that contained in the biscoumarin structure and amino acid residue.

The quenching observed in fluorescence studies for both compounds was characterized by molecular docking studies. In both structures, it was shown that the R groups of the benzene ring form hydrogen bonds with α_1-Arg141, on the side where compounds interact with β_2-Trp37. The three-dimensional location of the biscoumarins in their binding pocket inside hemoglobin is stabilized by the hydrogen bonding, or pi-pi interactions, which function as an anchor (Zhang et al. 2008). The primary forces behind the interaction between the biscoumarins and BHb were hydrophobic interactions and hydrogen bonds. In addition to these forces, the wan der Waals interaction of compound **B2** with the α1-Thr134 amino acid residue supported the dominant forces predicted from thermodynamic parameters in the previous section. Furthermore, docking results clarified the variations in the absorption and synchronous fluorescence studies, e.g., spectral shift in the synchronous fluorescence spectrum caused by **B1** and

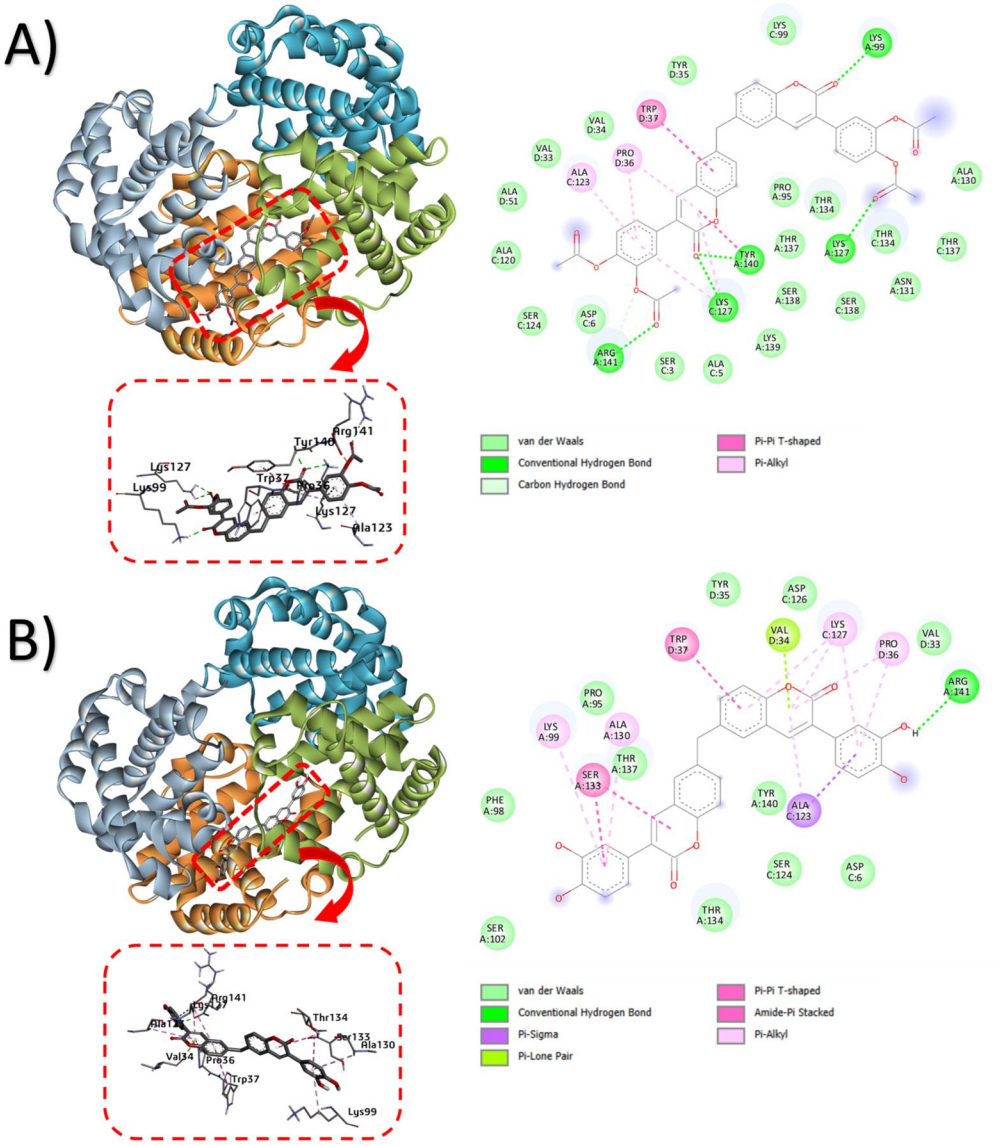

Figure 6. Dominant conformations of the (a) BHb-B1 and (b) BHb-B2 complexes with the minimum energy and interaction with amino acid residues obtained from molecular docking.

α1-Tyr140 interaction. Another illustration was the potential role of the **B2**-β_2-Val34 interaction in the increasing of the absorption Soret peak.

The stable biscoumarin conformations with BSA in three subdomains—the ones with the highest docking score conformation—types of these interactions are shown in Figure 5. The values of binding energy in the binding pockets of BSA are listed in Table 5. The most stable conformation of biscoumarins with the BSA was obtained in the IIIA subdomain of protein, where protein-ligand interactions take place inside this pocket. Similar to BHb interactions, most of the amino acid residues of BSA that take

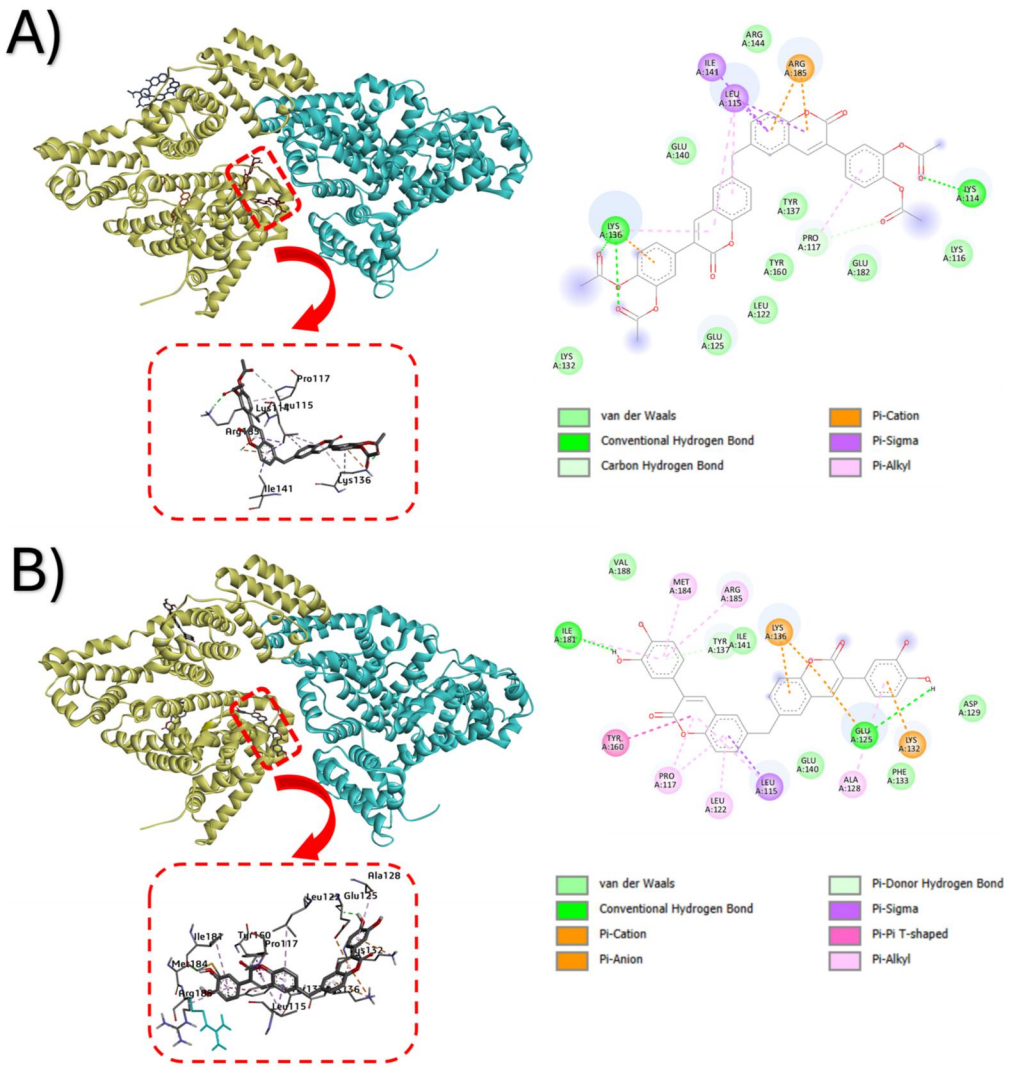

Figure 7. Dominant conformations of the (a) BSA-B1 and (b) BSA-B2 complexes with the minimum energy and interaction with amino acid residues obtained from molecular docking.

part in the binding process were the same, which include Lys132, Lys136, Glu125, Glu140, Tyr137, Pro117, Ile141, Leu115, and Pro117. In both structures, the pi electrons of the benzene ring formed pi-sigma interactions with same amino acid residue, Leu115.

Both biscoumarins are located in the close microenvironment of tyrosine residues, which also contribute to the intrinsic fluorescence of albumin. Therefore, we suggest that the shift in the fluorescence spectrum for **B1/B2** and the synchronized fluorescence spectrum for **B1** could be explained by these docking results. Both compounds formed hydrogen bonds through the carbonyl and -OH groups in the benzene ring substituted for the coumarin core, which was evidence that the structure was stabilized in the hydrophobic cavity of the IIIA subdomain of BSA by hydrogen bonds as well as van

Table 5. Binding energies of biscoumarin derivatives to BSA in different subdomains.

Compounds	Binding energy of site IB (kcal/mol)	Binding energy of site IIA (kcal/mol)	Binding energy of site IIIA (kcal/mol)
B1	+14.23	−3.44	−10.64
B2	−5.75	−7.80	−10.55

Table 6. Binding energies of biscoumarin derivatives to hemoglobin and albumin, calculated ligand efficiency values (LV), and observed interactions with residues.

Compounds	Binding energy (kcal/mol)	Binding energy (kj/mol)	*LV	Amino acid residues that interact with hydrogen bonds	Amino acid residues that make hydrophobic and other interactions
BHb-B1	−10.81	−45.25	−0.21	α_1-Lys99, α_1-Lys127, α_1-Tyr140, α_1-Arg141, β_1-Lys127	β_1-Ala123, β_2-Pro36, β_2-Trp37
BHb-B2	−9.47	−39.65	−0.24	α_1-Arg141	α_1-Lys99, α_1-Ala130, α_1-Ser133, α_1-Thr134, β_1-Ala123, β_1-Lys127, β_2-Val34, β_2-Pro36, β_2-Tr37
BSA-B1	−10.64	−44,52	−0.21	Lys114, Lys136, Pro117	Ile141, Leu115, Arg185, Pro117
BSA-B2	−10.55	−44.16	−0.27	Glu125, Ile181, Tyr137	Met184, Arg185, Tyr160, Pro117, Leu122, Leu115, Lys136, Ala128, Lys132,

*LV = Binding energy (kcal/mol)/Number of Heavy Atoms.

der Waals interactions. Unlike BHb, various pi-cation and pi-anion interactions were observed in both biscoumarins, and this bond type, which was more common in the **BSA-B2** complex, explained the electrostatic interactions obtained from thermodynamic parameters.

The values of binding energy and ligand efficiency for **BHb-B1/B2** and **BSA-B1/B2** complexes were also obtained from molecular docking results and summarized in Table 6. The theoretical ΔG° values were −39.65, −45.25, −44.52 and −44.16 kJ/mol for **BHb-B1, BHb-B2, BSA-B1** and **BSA-B2**, respectively. The docking scores were in agreement with the experimental ΔG° values obtained from fluorescence spectroscopy as shown in Table 4. In the light of this information, molecular docking studies strongly support the experimental results regarding complex formation biscoumarins with BHb and BSA. Therefore, it provides useful information about binding modes for a better understanding of protein-ligand interactions.

Conclusions

In this paper, we combined the multiple spectroscopic methods and molecular docking modeling to systematically investigate the interaction of BHb and BSA with the

biscoumarin derivatives identified as MAO enzyme inhibitors. Inhibitory activities of biscoumarins toward MAO-A and MAO-B were determined with IC_{50} values of 24.22 µM, 18.63 µM for **B1** and 1.8 µM, 3.75 µM for **B2**, respectively. Binding studies of **B1** and **B2** with BHb and BSA were carried out using absorption, fluorescence, synchronized fluorescence, and molecular docking methods. The quenching mechanisms of **B1** and **B2** with proteins were static from the absorption spectra, K_q, and K_{LB} values. Synchronous fluorescence revealed that the biscoumarins affected the Trp and Tyr residues microenvironments. **BSA-B2** was more stable toward other protein-ligand complexes according to the binding constants. Result of thermodynamic analysis demonstrated the binding was spontaneous and hydrogen bonds were dominant in all protein-ligand systems. All ligands binding with proteins were spontaneous and the hydrogen bonds were dominant based on thermodynamic analysis. Molecular docking has shown that both compounds make hydrophobic interactions with the *β*-Trp37 amino acid residues of BHb and stabilized *via* these interactions in the subdomain IIIA of BSA.

This study presents a comprehensive analysis elucidating the binding affinity and mode of interaction exhibited by biscoumarin derivatives with BHb and BSA. Examining interactions of potential pharmaceutical agents with proteins are important in providing information about the main forces that affect these interactions and determining the efficacy of drugs on biomacromolecular systems.

Disclosure statement

No potential conflicts of interest are reported by the authors.

Funding

This work was supported by Scientific and Technological Research Council of Turkey (TUBITAK) through 2209 A Project 2023-1 1919B012300697.

ORCID

Bengü Sema Mutafoğlu http://orcid.org/0009-0008-6767-1526
Furkan Meletli http://orcid.org/0000-0002-9126-0486
Özkan Danış http://orcid.org/0000-0003-1781-0520

References

Abdollahpour, N., V. Soheili, M. R. Saberi, and J. Chamani. 2016. Investigation of the interaction between human serum albumin and two drugs as binary and ternary systems. *European Journal of Drug Metabolism and Pharmacokinetics* 41 (6):705–21. doi: 10.1007/s13318-015-0297-y.

Alanazi, A. M., and A. S. Abdelhameed. 2016. A spectroscopic approach to investigate the molecular interactions between the newly approved irreversible ErbB blocker "Afatinib" and bovine serum albumin. *PloS One* 11 (1):e0146297. doi: 10.1371/journal.pone.0146297.

Ali, M. S., M. T. Rehman, H. Al-Lohedan, and M. F. AlAjmi. 2022. Spectroscopic and molecular docking investigation on the interaction of cumin components with plasma protein:

Assessment of the comparative interactions of aldehyde and alcohol with human serum albumin. *International Journal of Molecular Sciences* 23 (8):4078. doi: 10.3390/ijms23084078.

Anjomshoa, M., H. Hadadzadeh, S. J. Fatemi, and M. Torkzadeh-Mahani. 2015. A mononuclear Ni(II) complex with 5,6-diphenyl-3-(2-pyridyl)-1,2,4-triazine: DNA- and BSA-binding and anticancer activity against human breast carcinoma cells. *Spectrochimica Acta. Part A, Molecular and Biomolecular Spectroscopy* 136 Pt B:205–15. doi: 10.1016/j.saa.2014.09.016. 25315866

Basu, A., and G. Suresh Kumar. 2015. Binding of carmoisine, a food colorant, with hemoglobin: Spectroscopic and calorimetric studies. *Food Research International* 72:54–61. doi: 10.1016/j.foodres.2015.03.015.

Bawa, K., N. Deswal, A. Kumar, and R. Kumar. 2022. Scrutinzing the interaction of bovine serum albumin and human hemoglobin with isatin-triazole functionalized rhodamine through spectroscopic and in-silico approaches. *Journal of Molecular Liquids* 360 (119558):119558. doi: 10.1016/j.molliq.2022.119558.

Bekircan, O., Ö. Danış, M. E. Şahin, and M. Çetin. 2022. Monoamine oxidase A and B inhibitory activities of 3,5-diphenyl-1,2,4-triazole substituted [1,2,4]triazolo[3,4-b][1,3,4]thiadiazole derivatives. *Bioorganic Chemistry* 118:105493. doi: 10.1016/j.bioorg.2021.105493.

Bhuiya, S., S. Chowdhury, and S. Das. 2019. Molecular insight into the binding aspects of benzo[c]phenanthridine alkaloid nitidine with bovine hemoglobin: A biophysical exploration. *Spectrochimica Acta. Part A, Molecular and Biomolecular Spectroscopy* 223:117293. doi: 10.1016/j.saa.2019.117293.

BIOVIA. 2021. Dassault Systèmes, *Discovery Studio Visualizer*. San Diego, CA, USA: Dassault Systèmes. Accessed 30, July 2023. https://discover.3ds.com/discovery-studio-visualizer-download

Buddanavar, A. T., and S. T. Nandibewoor. 2017. Multi-spectroscopic characterization of bovine serum albumin upon interaction with atomoxetine. *Journal of Pharmaceutical Analysis* 7 (3): 148–55. doi: 10.1016/j.jpha.2016.10.001.

Chatterjee, S., and G. S. Kumar. 2016. Binding of fluorescent acridine dyes acridine orange and 9-aminoacridine to hemoglobin: Elucidation of their molecular recognition by spectroscopy, calorimetry and molecular modeling techniques. *Journal of Photochemistry and Photobiology. B, Biology* 159:169–78. doi: 10.1016/j.jphotobiol.2016.03.045.

Chowdhury, S., S. Bhuiya, L. Haque, and S. Das. 2020. In-depth investigation of the binding of flavonoid taxifolin with bovine hemoglobin at physiological pH: Spectroscopic and molecular docking studies. *Spectrochimica Acta. Part A, Molecular and Biomolecular Spectroscopy* 225: 117513. doi: 10.1016/j.saa.2019.117513.

Crane, E. A., and K. Gademann. 2016. Capturing biological activity in natural product fragments by chemical synthesis. *Angewandte Chemie* 55 (12):3882–902. doi: 10.1002/anie.201505863.

Dohare, N., M. A. Siddiquee, M. D. Parray, A. Kumar, R, and Patel, R. 2020. Esterase activity and interaction of human hemoglobin with diclofenac sodium: A spectroscopic and molecular docking study. *Journal of Molecular Recognition* 33 (8):e2841. doi: 10.1002/jmr.2841.

Edmondson, D. E., and C. Binda. 2018. "Monoamine oxidases", membrane protein complexes: Structure and function. *Sub-Cellular Biochemistry* 87:117–39. doi: 10.1007/978-981-10-7757-9_5.

Faisal, M., A. Saeed, D. Shahzad, T. A. Fattah, B. Lal, P. A. Channar, J. Mahar, S. Saeed, P. A. Mahesar, and F. A. Larik. 2017. Enzyme inhibitory activities an insight into the structure-activity relationship of biscoumarin derivatives. *European Journal of Medicinal Chemistry* 141 (141): 386–403. doi: 10.1016/j.ejmech.2017.10.009.

Farrugia, A. 2010. Albumin usage in clinical medicine: Tradition or therapeutic? *Transfusion Medicine Reviews* 24 (1):53–63. doi:.1016/j.tmrv.2009.09.005 doi: 10.1016/j.tmrv.2009.09.005.

Freed, J., and L. Chakrabarti. 2016. Defining a role for hemoglobin in Parkinson's disease. *NPJ Parkinson's Disease* 2 (1):16021. doi: 10.1038/npjparkd.2016.21.

Gaurav, M., A. Natesh, A. Arundhati, and D. Mariam. 2021. Biochemical aspects of hemoglobin-xenobiotic interactions and their implications in drug discovery. *Biochimie* 191:154–63. doi: 10.1016/j.biochi.2021.08.006.

Ghuman, J., P. A. Zunszain, I. Petitpas, A. A. Bhattacharya, M. Otagiri, and S. Curry. 2005. Structural basis of the drug-binding specificity of human serum albumin. *Journal of Molecular Biology* 353 (1):38–52. doi: 10.1016/j.jmb.2005.07.075.

Hanwell, M. D., D. E. Curtis, D. C. Lonie, T. Vandermeersch, E. Zurek, and G. R. Hutchison. 2012. Avogadro: An advanced semantic chemical editor, visualization, and analysis platform. *Journal of Cheminformatics* 4 (1):17. doi: 10.1186/1758-2946-4-17.

Hsieh, S. R., P. M. Reddy, C. J. Chang, A. Kumar, W. C. Wu, and H. Y. Lin. 2016. Exploring the behavior of bovine serum albumin in response to changes in the chemical composition of responsive polymers: Experimental and simulation studies. *Polymers* 8 (6):238. doi: 10.3390/polym8060238.

Hudáčová, M., S. Hamulaková, E. Konkoľová, R. Jendželovský, J. Vargová, J. Ševc, P. Fedoročko, O. Soukup, J. Janočková, V. Ihnatova, et al. 2021. Synthesis of new biscoumarin derivatives, in vitro cholinesterase inhibition, molecular modelling and antiproliferative effect in A549 human lung carcinoma cells. *International Journal of Molecular Sciences* 22 (8):3830. doi: 10.3390/ijms22083830.

Kaffash, M., S. Tolou-Shikhzadeh-Yazdi, S. Soleimani, S. Hoseinpoor, M. R. Saberi, and J. Chamani. 2024. Spectroscopy and molecular simulation on the interaction of Nano-Kaempferol prepared by oil-in-water with two carrier proteins: An investigation of protein-protein interaction. *Spectrochimica Acta. Part A, Molecular and Biomolecular Spectroscopy* 309: 123815. doi: 10.1016/j.saa.2023.123815.

Kaur, L., A. Singh, A. Datta, H, and Ojha, H. 2023. Multispectroscopic studies of binding interaction of phosmet with bovine hemoglobin. *Spectrochimica Acta. Part A, Molecular and Biomolecular Spectroscopy* 296:122630. doi: 10.1016/j.saa.2023.122630.

Lakowicz, J. R. 2006. *Principles of fluorescense spectroscopy*. 3rd ed. New York: Springer. doi: 10.1007/978-0-387-46312-4.

Lavanya, K., P. V. Babu, A. T. S. Bodapati, R. S. Reddy, S. R. Madku, B. K, and Sahoo, B. K. 2023. Binding of dicoumarol analog with DNA and its antioxidant studies: A biophysical insight by in-vitro and in-silico approaches. *International Journal of Biological Macromolecules* 244:125301. doi: 10.1016/j.ijbiomac.2023.125301.

Lehrer, S. S. 1971. Solute perturbation of protein fluorescence. Quenching of the tryptophyl fluorescence of model compounds and of lysozyme by iodide ion. *Biochemistry* 10 (17):3254–63. doi: 10.1021/bi00793a015.

Li, J. W., and J. C. Vederas. 2009. Drug discovery and natural products: End of an era or an endless frontier? *Science* 325 (5937):161–5. doi: 10.1126/science.1168243.

Liu, J., Y. He, D. Liu, Y. He, Z. Tang, H. Lou, Y. Huo, and X. Cao. 2018. Characterizing the binding interaction of astilbin with bovine serum albumin: A spectroscopic study in combination with molecular docking technology. *RSC Advances* 8 (13):7280–6. doi: 10.1039/c7ra13272g.

Liu, B., C. Yang, X. Yan, J. Wang, and Y. Lv. 2012. Interaction of avelox with bovine serum albumin and effect of the coexistent drugs on the reaction. *International Journal of Analytical Chemistry* 2012:408057. doi: 10.1155/2012/408057.

Lyndem, S., U. Hazarika, P. Athul, A. Bhatta, V. Prakash, A. N. Jha, and A. Singha Roy. 2023. A comprehensive in vitro exploration into the interaction mechanism of coumarin derivatives with bovine hemoglobin: Spectroscopic and computational methods. *Journal of Photochemistry and Photobiology A* 436 (114425):114425. doi: 10.1016/j.jphotochem.2022.114425.

Ma, F., C. Sun, W. Zhou, C. Xu, J. Zhou, G. Wang, and X. Yang. 2012. Investigation and comparison of bovine hemoglobin binding to Al13 and Al (III): Evidences from spectroscopic studies. *Spectrochimica Acta. Part A, Molecular and Biomolecular Spectroscopy* 97:885–91. doi: 10.1016/j.saa.2012.07.081.

Mishra, V., and R. J. Heath. 2021. Structural and biochemical features of human serum albumin essential for eukaryotic cell culture. *International Journal of Molecular Sciences* 22 (16):8411. doi: 10.3390/ijms22168411.

Morris, G. M., R. Huey, W. Lindstrom, M. F. Sanner, R. K. Belew, D. S. Goodsell, and A. J. Olson. 2009. Autodock4 and AutoDockTools4: Automated docking with selective receptor flexibility. *Journal of Computational Chemistry* 30 (16):2785–91. doi: 10.1002/jcc.21256.

Muratovıć, S., K. Durıć, E. Veljovıć, A. Osmanovıć, D. Softıć, and D. Zavrsnık. 2013. Synthesis of biscoumarin derivatives as antimicrobial agents. *Asian Journal of Pharmaceutical and Clinical Research* 6 (3):131–4.

Murray, R. D. H., J. Mendez, and S. A. Brown. 1982. *The natural coumarins occurrence, chemistry and biochemistry, Chichester*. New York: John Wiley and Sons. doi: 10.1111/1365-3040.ep11611630.

Novo, M., and W. Al-Soufi. 2007. Fluorescence study of the supramolecular interactions between coumarins and serum albumin. 11th International Electronic Conference on Synthetic Organic Chemistry (ECSOC 11), 1–30 November 2007.

Orhan, B. 2018. C¸es¸itli Arilkumarin Türevlerinin Glutatyon S-Transferaz Aktivitesi Üzerindeki Etkilerinin Incelenmesi., PhD diss., Marmara University Institute of Pure and Applied Sciences.

Osbourn, A. E., and V. Lanzottia. 2009. *Plant-derived natural products: Synthesis, function, and application*. Dordrecht, NL: Springer. doi: 10.1007/978-0-387-85498-4.

Ozalp, L., B. Orhan, M. M. Alparslan, F. Meletli, E. Çakmakçı, and Ö. Danış. 2023. Arylcoumarin and novel biscoumarin derivatives as potent inhibitors of human glutathione S-transferase. *Journal of Biomolecular Structure & Dynamics* 1–15. doi: 10.1080/07391102.2023.2262598.

Özdemir, N., and B. Özalp. 1995. Drag targeting with erythrocytes. *Journal of Faculty of Pharmacy of Ankara University* 24 (1):29–41. doi: 10.1501/Eczfak_0000000153.

Özdemir, Z., M. A. Alagöz, Ö. F. Bahçecioğlu, and S. Gök. 2021. Monoamine oxidase-B (MAO-B) inhibitors in the treatment of Alzheimer's and Parkinson's disease. *Current Medicinal Chemistry* 28 (29):6045–65. doi: 10.2174/0929867328666210203204710.

Peng, W., F. Ding, Y. K. Peng, and Y. Sun. 2014. Molecular recognition of malachite green by hemoglobin and their specific interactions: Insights from in silico docking and molecular spectroscopy. *Molecular bioSystems* 10 (1):138–48. doi: 10.1039/c3mb70416e.

Quds, R., M. Amiruddin Hashmi, Z. Iqbal, and R. Mahmood. 2022. Interaction of mancozeb with human hemoglobin: Spectroscopic, molecular docking and molecular dynamic simulation studies. *Spectrochimica Acta. Part A, Molecular and Biomolecular Spectroscopy* 280:121503. doi: 10.1039/c3mb70416e.

Ramsay, R. R., and A. Albreht. 2018. Kinetics, mechanism, and inhibition of monoamine oxidase. *Journal of Neural Transmission* 125 (11):1659–83. doi: 10.1007/s00702-018-1861-9.

Seal, P., J. Sikdar, N. Ghosh, P. Biswas, and R. Haldar. 2019. Exploring the binding dynamics of etoricoxib with human hemoglobin: A spectroscopic, calorimetric, and molecular modeling approach. *Journal of Biomolecular Structure & Dynamics* 37 (11):3018–28. doi: 10.1080/07391102.2018.1508369.

Seal, P., J. Sikdar, A. Roy, and R. Haldar. 2017. Acetaminophen interacts with human hemoglobin: Optical, physical and molecular modeling studies. *Journal of Biomolecular Structure & Dynamics* 35 (6):1307–21. doi: 10.1080/07391102.2016.1180262.

Seal, P., J. Sikdar, A. Roy, and R. Haldar. 2018. Binding of ibuprofen to human hemoglobin: Elucidation of their molecular recognition by spectroscopy, calorimetry, and molecular modeling techniques. *Journal of Biomolecular Structure & Dynamics* 36 (12):3137–54. doi: 10.1080/07391102.2017.1384399.

Shahabadi, N., M. Maghsudi, Z. Kiani, and M. Pourfoulad. 2011. Multispectroscopic studies on the interaction of 2-tert-butylhydroquinone (TBHQ), a food additive, with bovine serum albumin. *Food Chemistry* 124 (3):1063–8. doi: 10.1016/j.foodchem.2010.07.079.

Shanmugaraj, K., S. Anandakumar, and M. Ilanchelian. 2014. Exploring the biophysical aspects and binding mechanism of thionine with bovine hemoglobin by optical spectroscopic and molecular docking methods. *Journal of Photochemistry and Photobiology. B, Biology* 131:43–52. doi: 10.1016/j.jphotobiol.2014.01.001.

Taheri, R., N. Hamzkanlu, Y. Rezvani, S. Niroumand, F. Samandar, Z. Amiri-Tehranizadeh, M. R. Saberi, and R. Chamani. 2022. Exploring the HSA/DNA/lung cancer cells binding behavior of p-Synephrine, a naturally occurring phenyl ethanol amine with anti-adipogenic activity: Multi spectroscopic, molecular dynamic and cellular approaches. *Journal of Molecular Liquids* 368 (B):120826. doi: 10.1016/j.molliq.2022.120826.

Tan, Y. Y., P. Jenner, and S. D. Chen. 2022. Monoamine oxidase-B inhibitors for the treatment of Parkinson's disease: Past, present, and future. *Journal of Parkinson's Disease* 12 (2):477–93. doi: 10.3233/JPD-212976.

Topală, T., A. Bodoki, L. Oprean, and R. Oprean. 2014. Bovine serum albumin interactions with metal complexes. *Clujul Medical (1957)* 87 (4):215–9. doi: 10.15386/cjmed-357.

Tunç, S., O. Duman, and B. K. Bozoğlan. 2013. Studies on the interactions of chloroquine diphosphate and phenelzine sulfate drugs with human serum albumin and human hemoglobin proteins by spectroscopic techniques. *Journal of Luminescence* 140:87–94. doi: 10.1016/j.jlumin.2013.03.015.

Wang, L., R. Liu, Z. Chi, B. Yang, P. Zhang, and M. Wang. 2010. Spectroscopic investigation on the toxic interactions of Ni2+ with bovine hemoglobin. *Spectrochimica Acta. Part A, Molecular and Biomolecular Spectroscopy* 76 (2):155–60. doi: 10.1016/j.saa.2010.03.006.

Yamasaki, K., V. T. Chuang, T. Maruyama, and M. Otagiri. 2013. Albumin-drug interaction and its clinical implication. *Biochimica et Biophysica Acta* 1830 (12):5435–43. doi: 10.1016/j.bbagen.2013.05.005.

Yang, A. P., M. H. Ma, X. H. Li, and M. Y. Xue. 2012. Interaction of irbesartan with bovine hemoglobin using spectroscopic techniques and molecular docking. *Spectroscopy* 27 (2):119–28. doi: 10.1155/2012/136287.

Yeshi, K., D. Crayn, E. Ritmejerytė, and P. Wangchuk. 2022. Plant secondary metabolites produced in response to abiotic stresses has potential application in pharmaceutical product development. *Molecules* 27 (1):313. doi: 10.3390/molecules27010313.

Yu, X., X. Cai, S. Li, L. Luo, J. Wang, M. Wang, and L. Zeng. 2022. Studies on the interactions of theaflavin-3,3'-digallate with bovine serum albumin: Multi-spectroscopic analysis and molecular docking. *Food Chemistry* 366:130422. doi: 10.1016/j.foodchem.2021.130422.

Yuce-Dursun, B., Ö. Danış, L. Ozalp, E. Sahin, S. Demir, S. S. Erdem, and A. Ogan. 2023. In vitro and in silico investigation of inhibitory activities of 3-arylcoumarins and 3-phenylazo-4-hydroxycoumarin on MAO isoenzymes. *Structural Chemistry* 34 (5):1715–29. doi: 10.1007/s11224-022-02092-x.

Yu, Q., M. Li, H. Chen, L. Xu, J. Cheng, G. Lin, Y. Liu, Z. Su, X. Yang, Y. Li, et al. 2022. The discovery of berberine erythrocyte-hemoglobin self-assembly delivery system: A neglected carrier underlying its pharmacokinetics. *Drug Delivery* 29 (1):856–70. doi: 10.1080/10717544.2022.2036870.

Zhang, H. M., Z. H. Fei, B. P. Tang, J. Chen, W. H. Tao, and Y. Q. Wang. 2012. The interaction of blood proteins with brucine. *Molecular Biology Reports* 39 (4):4937–47. doi: 10.1007/s11033-011-1289-x.

Zhang, Y., Y. Li, L. Dong, J. Li, W. He, X. Chen, and Z. Hu. 2008. Investigation of the interaction between naringin and human serum albumin. *Journal of Molecular Structure* 875 (1–3):1–8. doi: 10.1016/j.molstruc.2007.03.063.

Zolghadri, S., A. A. Saboury, E. Amin, and A. A. Moosavi-Movahedi. 2010. A spectroscopic study on the interaction between ferric oxide nanoparticles and human hemoglobin. *Journal of the Iranian Chemical Society* 7 (S2):S145–S153. doi: 10.1007/BF03246193.